Rept. 510-IF, Vol. 1, Dec. 1976.
14. W. P. Chamberlin and D. E. Amsler. A Pilot Field Study of Concrete Pavement Texturing Methods. HRB, Highway Research Record 389, 1972, pp. 5-17.
15. W. P. Chamberlin. Concrete Pavement Texturing Methods—A Review of Experience in New York. Engineering R&D Bureau, New York State Department of Transportation, Feb. 1978.
16. R. R. Hegmon. Seasonal Variations in Pavement Skid Resistance—Are They Real? Public Roads, Vol. 42, No. 2, Sept. 1978.

Authors' Closure

We would like to express our appreciation to Chamberlin for making available additional data in support of one aspect of our research. Chamberlin's regression coefficients of 4.53 and 0.497 are in good agreement with ours of 4.10 and 0.47 respectively, considering the precision of the correlated data (SN_{40} and mean depth measured by the sand-patch method). Research that will consider 20 sites in Pennsylvania is planned for 1979, so we would welcome similar data from others.

Equation 19 eliminates the parameter SN_0 from our model (Equation 13). We have found that this parameter is affected by both microtexture and short-term variations in weather. Weather-related effects are eliminated by conducting all skid measurements in one weather area at the same time. However, it is probably not possible to compare data sets taken at different locations at different times without correcting for weather-related factors such as rainfall history. The differences between Equations 16 and 17 can be attributed in part to these effects, and larger differences might be expected. Research into seasonal and short-term variations is under way and, if it is successful, we may be able to account for microtexture and weather in a generalized model.

Publication of this paper sponsored by Committee on Surface Properties-Vehicle Interaction.

Determination of Skid Resistance-Speed Behavior and Side Force Coefficients of Pavements

V. R. Shah, Dorr-Oliver Company, Stamford, Connecticut
J. J. Henry, Pennsylvania State University

Pavement friction characteristics including skid resistance-speed dependence, side force coefficients, and brake slip numbers are seen to be derivable from data obtained in the transient slip test. The transient slip test is described, and it is noted that any friction tester with force-measuring transducers can be used for these measurements. The brake slip numbers are shown to be independent of the rate of wheel lockup, which leads to the observation that brake slip numbers obtained during a transient slip test are equivalent to locked-wheel skid numbers at the same sliding speed. Side force coefficients can be computed from transient slip data with the help of a model. The data and conclusions apply to the standard skid-test tire operating under fixed test conditions and normal load, water film thickness, and inflation pressure.

Highway safety in the United States is currently evaluated by using locked-wheel skid numbers (1). During the lifetime of a pavement wearing course, the skid number (SN) is measured at least once a year at a single vehicle speed—usually 65 km/h (40 mph)—although sometimes at the "prevailing traffic speed." Because vehicles are operated on highways at a variety of speeds and only rarely in the locked-wheel mode, the ranking of pavement safety by means of a locked-wheel test at a single speed can be questioned. Furthermore, vehicles require adequate lateral forces to maintain directional stability in cornering maneuvers. In a complete evaluation of pavement safety, it is necessary to measure the complete frictional characteristics of a pavement at various speeds, cornering angles, and wheel stop rates. It would clearly be impractical to do this for each pavement in the country on an annual basis.

Research was initiated at the Pennsylvania Transportation Institute (PTI), Pennsylvania State University, to determine the degree of interrelationship among slip, side force, and locked-wheel data (2,3). The objective of this research was to determine the most efficient means of evaluating the frictional capability of pavements. As a result of this research, a methodology was developed for processing data from a single measurement at one vehicle speed to obtain the speed dependence and side force frictional characteristics of a pavement.

EXPERIMENTAL PROCEDURE

The Penn State Mark III Road Friction Tester (4) was used in this study. The tester has a single wheel, a six-component force-torque measuring hub, and a hydraulic system that can steer the test wheel into angles of up to 12° in relation to the forward velocity of the towing vehicle. Two rotary variable differential transformers measure the angle of the test trailer and the angle of the free-trailing fifth wheel relative to the truck axis. In this way, the actual yaw angle of the test trailer—including the correction for any yaw it induces in the

direction of the towing vehicle—is determined. Both the test-wheel and fifth-wheel speeds are measured. All signals are recorded on an oscillograph recorder that has sufficient response so that friction force and velocities can be recorded as the test tire is being locked up. In addition, side force and yaw angle can be recorded as the trailer sweeps from free trailing to a 12° yaw angle at a rate of about 24°/s.

The pavements used in this study (six sites at the PTI Skid Test Facility) are described below:

Pavement	Type
3	Dense-graded asphalt concrete with thick application of Jennite and low-friction surface
4	Dense-graded asphalt concrete with a sand-epoxy overlay and fine-grained texture
5	Portland cement concrete lightly dragged in transverse direction with burlap drag
6	Dense-graded asphalt concrete (Pennsylvania Specification 1D2A)
8	Open-graded asphalt concrete with river bottom gravel aggregate (Pennsylvania Specification SR1A)
Tangent	Dense-graded asphalt concrete (same as site 6 but subjected to wear as part of PTI Pavement Durability Track)

Some supporting data were also obtained on public roads in the State College, Pennsylvania, area.

Three test tires were included in the study: the ASTM E 249 five-ribbed tire (5), the ASTM E 501 seven-ribbed tire (6), and the ASTM E 524 blank tire (7). Data are reported here only for the E 501 seven-ribbed tire, which is the current standard test tire. Data for the other tires are given elsewhere (3).

In all tests, the on-board watering system delivered a nominal 0.50-mm (0.02-in) water film thickness. Tire inflation pressure was 165 kPa (24 lbf/in^2) (measured cold), and the vertical load was 4670 N (1050 lb).

Locked-wheel skid numbers were obtained at 16, 24, 32, 48, 64, and 80.5 km/h (10, 15, 20, 30, 40, and 50 mph). Side force coefficients with a free rolling wheel were obtained at yaw angles up to 12°. Transient slip data were obtained at 48, 64, and 80.5 km/h. The test procedure for transient slip consists of operating the strip chart recorder fast enough so that the friction force can be read as a function of the rotational velocity of the test tire from the free rolling to the fully locked condition. In all other respects, this test is the same as a locked-wheel test. The lockup rates for the road friction tester are between 0.25 and 0.5 for the pavements tested.

Because all data reported here were collected during the first two weeks of August 1975, seasonal variations and their possible effects on the data are not considered.

TEST RESULTS

In the procedure used in this research, the locked-wheel skid number (SN) is the special case of the transient slip brake slip number (BSN) at 100 percent slip. The BSN is the ratio of friction force to normal load multiplied by 100 at a specified wheel slip. Percentage slip is defined as the deficiency in angular velocity caused by braking expressed as a percentage of free-rolling angular velocity. Any skid tester equipped with a force-measuring hub and sufficiently responsive instrumentation can be used to obtain data on transient slip.

The BSN is a function of the percentage slip and the test speed. In other investigations of the effect of lockup rate, it has been found that peak and slide coefficients are not significantly affected by lockup from 0.25 to 1 s (8). Some tests were performed by using a constant slip tester on loan from the Federal Aviation Agency (9). At the same time, data were obtained with the road friction tester on the transient slip mode. The constant slip test has an effective zero lockup rate compared with the rapid lockup rate of the transient slip test. Figure 1 shows the results of these tests. The slight difference in the results can be attributed to the calibration of the two testers. The effect of wheel lockup rate is therefore considered to be negligible.

A significant discovery resulted from plotting the BSN data versus sliding speed rather than percentage slip. Sliding speed can be determined by multiplying the percentage slip by the test speed and represents the velocity of the tire tread relative to the pavement. Locked-wheel data can also be plotted on these coordinates because SN is equivalent to BSN at 100 percent slip. Figures 2 through 7 show the plots for reduced

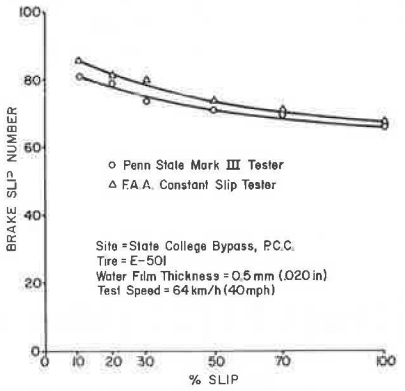

Figure 1. Brake slip number versus percentage slip for constant and variable speed testers.

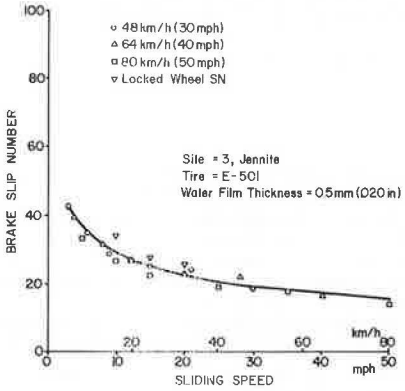

Figure 2. Reduced brake slip number versus sliding speed for site 3.

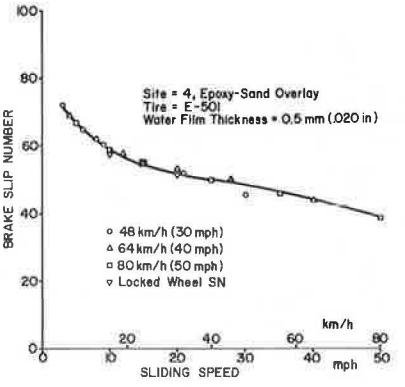

Figure 3. Reduced brake slip number versus sliding speed for site 4.

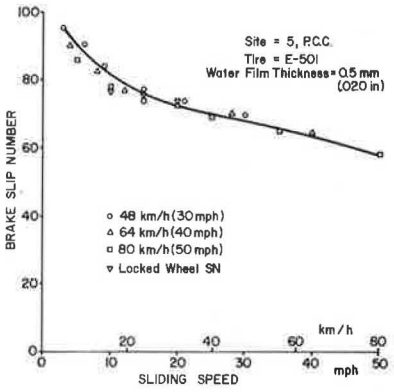

Figure 4. Reduced brake slip number versus sliding speed for site 5.

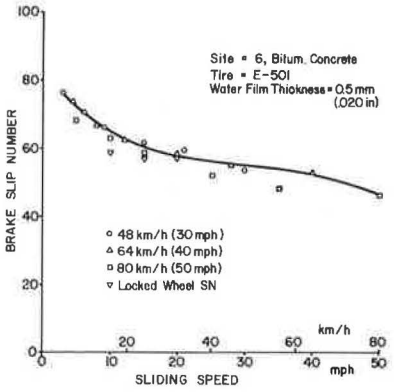

Figure 5. Reduced brake slip number versus sliding speed for site 6.

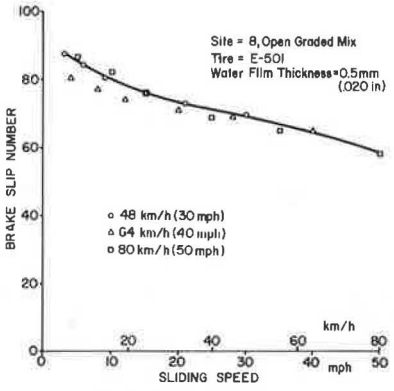

Figure 6. Reduced brake slip number versus sliding speed for site 8.

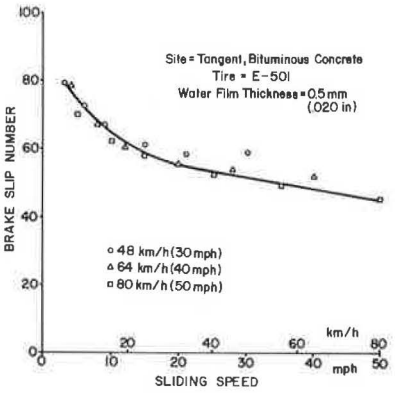

Figure 7. Reduced brake slip number versus sliding speed for site tangent.

brake slip number (BSN versus sliding speed) for the six test sites. Each datum point for the transient slip data represents the average of at least 15 measurements; the low-speed locked-wheel data are averages of five measurements.

A single curve drawn through the data in the plots of reduced brake slip number can be used to determine the speed-related friction performance of a pavement. For example, a locked-wheel test at 48 km/h (30 mph) will produce the same result for SN_{30} as a transient slip test result at 80.5 km/h (50 mph) with 60 percent slip. The curves for reduced brake slip number can be obtained from transient slip tests at a single test speed and used to determine the skid number-speed behavior up to that test speed.

Prediction of Side Force Coefficients From Transient Slip Data

A model designed to predict side forces generated by a cornering tire requires parameters that describe the behavior of the tire and the friction force in the tire-pavement contact area as a function of sliding speed. The friction forces depend on the combination of tire and pavement and can be measured by the transient slip method described above. The other parameters, those that describe the tire, depend on the tire only and are thus fixed when the tire is selected. It is possible then to predict side force coefficients (the ratio of the lateral force on a cornering tire to the normal load times 100) for a given tire given the reduced brake slip number plot for that tire-pavement combination.

The following assumptions were made for the model:

1. The tire behaves as an elastic beam representing the tread base, supported on an elastic foundation represented by the carcass, which permits simulation of vertical and longitudinal carcass motion.
2. A pressure distribution in the tire contact region is parabolic along the contact length and uniform across it.
3. The contact region is approximated by a rectangle.
4. The friction coefficient is isotropic.
5. The carcass has a bending stiffness EI.

In general, the tire motion during braking, traction, or cornering is a combination of slipping, sliding, and rolling. The tire-pavement contact surface can be divided into sliding and nonsliding regions, which are analyzed separately. The coordinate system defined here is similar to the one adopted by the Society of Automotive Engineers (10) except that the system discussed here takes into account finite deformation of a tire in the region of contact with the pavement. Figure 8 shows the coordinate system for a freely rolling, yawed tire. The analysis is an extension of analyses

Figure 8. Coordinate axes for tire model.

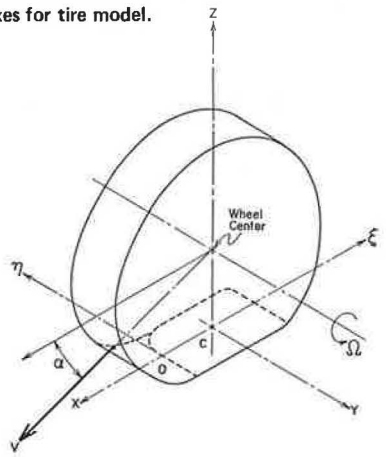

made by Fiala (11) and Sakai (12), which do not account for the dependence of friction on speed and are valid only for small yaw angles.

Nonsliding Region

Figure 9 shows the shear deformation of a single portion of the tire tread for a freely rolling, yawed tire. (Deformation and shear stress are averaged across the tire tread, and the resulting kinematic and force expressions depend on the ξ coordinate only.) In Figure 9, B is a point on the carcass whereas A is a corresponding point on the tread element that is in contact with the road surface. O represents the leading edge of the tire in contact with the road surface. The diagram of tire velocity shown in Figure 8 shows the wheel yawed at an angle α to the direction of motion. It can be seen in the figure that V_r represents the free-rolling velocity of the tire whereas V_y represents the lateral elastic slip or slide of the tire. In time t, the base point B of a tread element will move into the contact region a longitudinal distance ξ as determined by rolling velocity V_r.

Then,

$$\xi = -V_r \cdot t \tag{1}$$

where V_r is in the negative ξ direction. The velocity of the contacting tip A is V. During the same time interval t, A will be laterally displaced by a distance given by

$$\eta = -V_y \cdot t \tag{2}$$

t can be eliminated between Equations 1 and 2 to give

$$\eta = (V_y/V_r) \cdot \xi \tag{3}$$

The preceding analysis assumes that there is no sliding or slipping of the tire with respect to the road surface. In the region of adhesion, lateral deformation is produced by the static coefficient of friction with a limiting value μ°. The friction force required to produce this displacement depends on the lateral stiffness of the element (C_y in pounds force per cubic inch) (because the equations were formulated in U.S. customary units, no SI equivalents are given). The force per unit area is

$$F_\eta = C_y (\eta - \eta_b) \tag{4}$$

where η_b is the carcass deformation.

The maximum static friction force available from a particular tire-pavement combination depends on the limiting friction coefficient (μ°) and the vertical contact pressure distribution (P_z). Friction force varies linearly until the limiting condition is reached when

$$F_\eta/(\xi = \xi_a) = \mu^\circ P_z/(\xi = \xi_a) \tag{5}$$

where ξ_a is the limit of the adhesion region.

The curve of carcass deflection is given by Hartranft (4):

$$\eta_b = bS \cdot (\xi/L)[1 - (\xi/L)] \tag{6}$$

where b is the beam constant (0.015×10^{-3} in/lbf for the E 501 tire) determined experimentally according to the Hartranft procedure (4) and S is the side force. Assuming a parabolic pressure distribution in the contact region gives

$$P_z = (6N/wL^2) \cdot (\xi/L)[1 - (\xi/L)] \tag{7}$$

where

- N = static wheel load (1050 lbf for the tests reported here);
- w = tire contact patch width, the width of the tire minus the total width of the grooves (4.62 in for the E 501 tire); and
- L = tire contact patch length (6 in for the E 501 tire).

At the point of incipient slip,

$$\xi = \xi_a \tag{8}$$

Substituting for F_η and R_z in Equation 5 from Equations 4 and 7 gives

$$C_y (\eta - \eta_b) = (6\mu^\circ N/wL^2) \cdot (\xi_a/L)[1 - (\xi_a/L)] \tag{9}$$

But $\eta = \xi_a \tan \alpha$. Substituting for η and η_b and solving the expression for ξ_a give

$$\xi_a = [(6\mu^\circ N/wL^2 C_y) + (bS/L) - \tan \alpha] \cdot [(L/6\mu^\circ N/wL^2 C_y) + (bS/L)] \tag{10}$$

Sliding Region

Beyond the adhesion limit, the tread element begins to slide back to its original undeformed position and the sliding velocity changes from zero at the limiting adhesion point to its maximum at the exit of the contact region. The side force per unit area in this region is given by

$$F_\eta = \mu P_z \tag{11}$$

The total side force S is given by

$$S = S_{adhesion} + S_{sliding} \tag{12}$$

which can be obtained by integrating over the entire contact region. Thus,

$$S = \int_0^{\xi_a} w \cdot F_\eta \cdot d\xi + \int_{\xi_a}^{L} w \cdot \mu p_z \cdot d\xi \tag{13}$$

Substituting for F_η and P_z and simplifying give

$$S = ([\tfrac{1}{2} \cdot w \cdot C_y \cdot \xi_a^2 \cdot \tan \alpha] + \{\mu N[1 - 3(\xi_a/L)^2 \; 2(a/L)^3]\})/ \{1 + (b/L)\xi_a^2 [\tfrac{1}{2} - (\xi_a/3L)]\, w C_y\} \tag{14}$$

where the first term in the numerator represents the contribution by the adhesion region and the second the contribution by the sliding region. Thus, the expres-

Figure 9. Tire deformation in the contact patch.

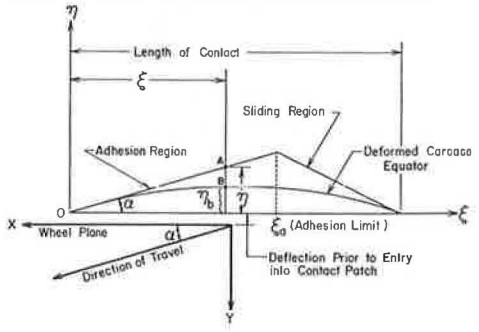

sion for S permits evaluation of S for any yaw angle α. μ is a function of sliding velocity and can be obtained from plots for BSN and sliding speed. In the present case, values are obtained from Figures 2 to 7 for the particular surfaces.

C_y can be obtained as follows: In the adhesion region, the side force is given by

$$S = S_{adhesion} = \tfrac{1}{2} \cdot w \cdot C_y \cdot \xi_a^2 \cdot \tan \alpha \quad (15)$$

For the limiting condition of α approaching zero, this expression becomes

$$S = \tfrac{1}{2} \cdot w \cdot C_y \cdot \xi_a^2 \cdot \alpha \quad (16)$$

and

$$(\partial S/\partial \alpha) = \tfrac{1}{2} \cdot w \cdot C_y \cdot \xi_a^2 \quad (17)$$

But ξ_a = L = contact length (in that no slip takes place in this condition), which gives

$$(\partial S/\partial \alpha) = \tfrac{1}{2} \cdot w \cdot C_y \cdot L^2 \quad (18)$$

$$C_y = 2(\partial S/\partial \alpha)/w \cdot L^2 \quad (19)$$

From the experimentally obtained plots of side force versus yaw angle, the value of $\partial S/\partial \alpha$ at α approaching zero was calculated. This gives C_y = 250 lbf/in^3 for the E 501 tire. The length of the contact region was determined by obtaining tire footprints under statically loaded conditions. The values of side force obtained from Equation 14 are compared with the experimentally obtained results for the six test sites in Figures 10 to 15.

Figure 10. Side force coefficient versus yaw angle for site 3.

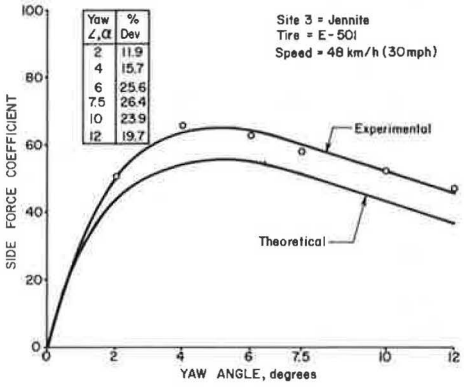

Figure 11. Side force coefficient versus yaw angle for site 4.

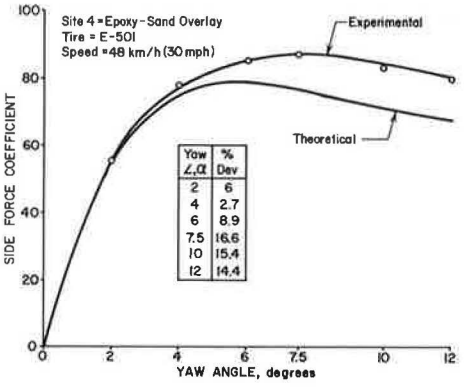

Figure 12. Side force coefficient versus yaw angle for site 5.

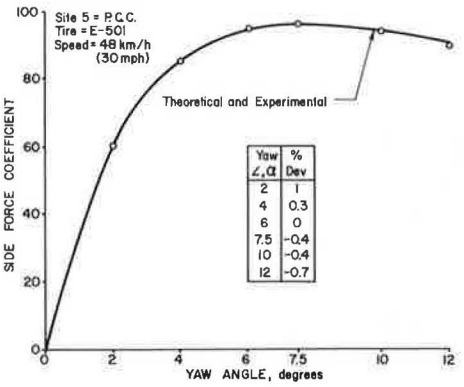

Figure 13. Side force coefficient versus yaw angle for site 6.

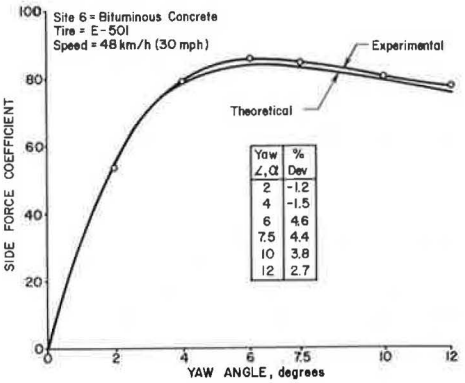

Figure 14. Side force coefficient versus yaw angle for site 8.

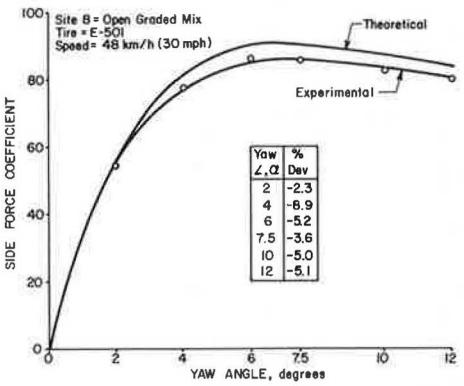

Figure 15. Side force coefficient versus yaw angle for site tangent.

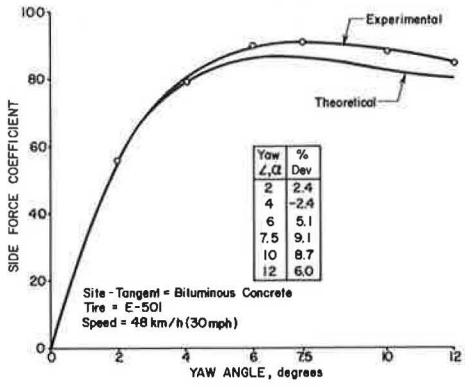

The results show a good agreement between experimental and theoretical results for sites 5, 6, 8, and tangent but poorer agreement for sites 3 and 4. The cause of this poor agreement lies in the assumption that the friction coefficient is isotropic. Although it is not possible to obtain SNs perpendicular to the direction of travel, the British Portable Tester (13) was used to determine British portable numbers (BPNs) in relation to direction of travel to determine whether the assumption of isotropic friction is valid. The results obtained are given in the table below, which shows that the assumption is least valid for sites 3 and 4:

	BPN		
Site	Parallel to Road	Perpendicular to Road	Deviation (%)
3	53.2	58.4	+9.8
4	65	70.3	+8.2
5	86	83	-3.5
6	81	81	0
8	82.1	81.7	-0.5

Thus, the calculated results for these sites would be expected to differ from experimental results and, because friction is greater in the lateral direction, the experimental results are greater than the predictions.

CONCLUSIONS

It has been shown that collecting data during the transient portion of a locked-wheel skid test as the test tire undergoes the transition from freely rolling to fully locked can provide useful information. During the transition, instantaneous friction force and corresponding sliding speed (relative velocity of the tread and the pavement) can be measured and are found to be independent of test speed and wheel lockup rate. Data on brake slip number and sliding speed characterize the relation between pavement friction and speed and can be used, with the help of a model, to determine side force coefficients.

Transient slip tests do not require unique equipment. Any locked-wheel skid tester provided with a force-measuring hub and instrumentation that has sufficient response to measure forces and angular velocities during the transition can be used.

ACKNOWLEDGMENTS

This research was sponsored by the Pennsylvania Department of Transportation and the Federal Highway Administration. We would like to express our gratitude to R. K. Shaffer and R. R. Hegmon of those agencies for their cooperation in project coordination and for their constructive criticism and guidance during the conduct of this work. Consultation with and the suggestions of W. E. Meyer of Pennsylvania State University provided a valuable contribution to the project. The contents and the conclusions of this presentation do not necessarily reflect the opinion of the sponsors.

REFERENCES

1. Standard Test Method for Skid Resistance of Paved Surfaces Using a Full-Scale Tire. Annual Book of ASTM Standards, Pt. 15, E 274-70, 1977.
2. J. J. Henry and W. E. Meyer. Relationship of Locked Wheel Friction to That of Other Test Modes. Bureau of Materials, Testing and Research, Pennsylvania Department of Transportation, 1975.
3. V. R. Shah and J. J. Henry. Relationship of Locked Wheel Friction to That of Other Test Modes. Bureau of Materials, Testing and Research, Pennsylvania Department of Transportation, Final Rept. 72-7, March 1977.
4. T. J. Hartranft. Theoretical and Experimental Correlation Between Locked Wheel and Other Friction Modes. Pennsylvania State Univ., PTI Rept. 7502, Feb. 1975.
5. Specification for Standard Tire for Pavement Tests (Discontinued 1973). Annual Book of ASTM Standards, Pt. 15, E 249, 1973.
6. Standard Specification American Tire for Pavement Skid-Resistance Tests. Annual Book of ASTM Standards, Pt. 15, E 501, 1977.
7. Standard Specification for Smooth-Tread Standard Tire for Special-Purpose Pavement Skid-Resistance Tests. Annual Book of ASTM Standards, Pt. 15, 1977.
8. J. L. Bradisse, A. F. Ramsey, and S. R. Sacia. Mobile Truck Tire Test System. SAE, Paper 741138, 1974.
9. W. A. Hiering and C. R. Grisel. Friction Effects Due to Runway Grooving. Federal Aviation Agency, U.S. Department of Transportation, Interim Rept. on Project 510-003-07X, 1968.
10. Vehicle Dynamic Technology. SAE, Recommended Practice J670C, Handbook Supplement, Jan. 1973.
11. E. Fiala. Seitenkräfte am Rollenden Luftreifen. Zeitschrift des Vereins Deutscher Ingenieure, No. 29, Oct. 1974.
12. H. Sakai. Theoretical Study of the Effect of Tractive and Braking Forces on the Cornering Characteristics of a Tire. Safety Research Tour in the U.S.A., Bulletin, Japan Society of Automotive Engineers, No. 3, Paper 4, March 1971, 1969, pp. 64-74.
13. Standard Test Method for Measuring Pavement Surface Frictional Properties Using the British Portable Tester. Annual Book of ASTM Standards, Pt. 15, E 303, 1977.

Publication of this paper sponsored by Committee on Surface Properties-Vehicle Interaction.